Article

Cell Chemical Biology

Synthesis and Degradation of Adenosine 5′-Tetraphosphate by Nicotinamide and Nicotinate Phosphoribosyltransferases

Graphical Abstract

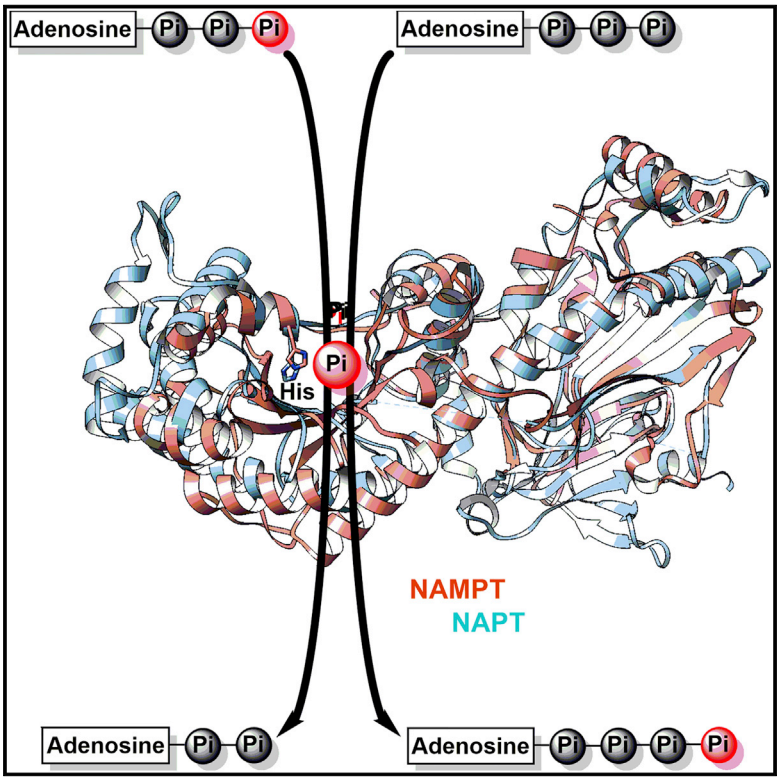

Highlights

- Ap4 is identified as a novel ATP-derived product of NAMPT and NAPT
- A phosphor-transfer mechanism for reversible synthesis of Ap4 from ATP is proposed
- The FK866-inhibited NAMPT enzyme still catalyzes Ap4 synthesis
- A correlation between NAMPT and Ap4 levels in murine cells and plasma is observed

Authors

Adolfo Amici, Ambra A. Grolla, Erika Del Grosso, ..., Silverio Ruggieri, Armando A. Genazzani, Giuseppe Orsomando

Correspondence

armando.genazzani@uniupo.it (A.A.G.), g.orsomando@univpm.it (G.O.)

In Brief

Amici et al. present a novel phosphor-transfer reaction catalyzed by NAMPT and NAPT, two key enzymes for NAD biosynthesis. This property allows NAMPT to regulate in vivo adenosine 5-tetraphosphate (Ap4) levels, thus conferring an unpredicted signaling role to this enzyme.

Amici et al., 2017, Cell Chemical Biology *24*, 553–564
May 18, 2017
http://dx.doi.org/10.1016/j.chembiol.2017.03.010

CellPress

Cell Chemical Biology
Article

Synthesis and Degradation of Adenosine 5′-Tetraphosphate by Nicotinamide and Nicotinate Phosphoribosyltransferases

Adolfo Amici,[1,4] Ambra A. Grolla,[2,4] Erika Del Grosso,[2] Roberta Bellini,[2] Michele Bianchi,[2] Cristina Travelli,[2] Silvia Garavaglia,[2] Leonardo Sorci,[1] Nadia Raffaelli,[3] Silverio Ruggieri,[3] Armando A. Genazzani,[2,*] and Giuseppe Orsomando[1,5,*]

[1]Department of Clinical Sciences, Section of Biochemistry, Polytechnic University of Marche, Via Ranieri 67, 60131 Ancona, Italy
[2]Department of Pharmaceutical Sciences, Università del Piemonte Orientale, Via Bovio 6, 28100 Novara, Italy
[3]Department of Agricultural, Food and Environmental Sciences, Polytechnic University of Marche, Via Brecce Bianche 10, 60131 Ancona, Italy
[4]Co-first author
[5]Lead Contact
*Correspondence: armando.genazzani@uniupo.it (A.A.G.), g.orsomando@univpm.it (G.O.)
http://dx.doi.org/10.1016/j.chembiol.2017.03.010

SUMMARY

Adenosine 5'-tetraphosphate (Ap4) is a ubiquitous metabolite involved in cell signaling in mammals. Its full physiological significance remains unknown. Here we show that two enzymes committed to NAD biosynthesis, nicotinamide phosphoribosyltransferase (NAMPT) and nicotinate phosphoribosyltransferase (NAPT), can both catalyze the synthesis and degradation of Ap4 through their facultative ATPase activity. We propose a mechanism for this unforeseen additional reaction, and demonstrate its evolutionary conservation in bacterial orthologs of mammalian NAMPT and NAPT. Furthermore, evolutionary distant forms of NAMPT were inhibited in vitro by the FK866 drug but, remarkably, it does not block synthesis of Ap4. In fact, FK866-treated murine cells showed decreased NAD but increased Ap4 levels. Finally, murine cells and plasma with engineered or naturally fluctuating NAMPT levels showed matching Ap4 fluctuations. These results suggest a role of Ap4 in the actions of NAMPT, and prompt to evaluate the role of Ap4 production in the actions of NAMPT inhibitors.

INTRODUCTION

Nicotinamide phosphoribosyltransferase (NAMPT) and nicotinate phosphoribosyltransferase (NAPT) are structurally similar NAD biosynthetic enzymes belonging to the class of dimeric type II phosphoribosyltransferases (PRTases) (Marletta et al., 2015). They bind nicotinamide (Nam) or nicotinic acid (Na) as the respective substrate, catalyzing their reversible transfer to the ribose 5-phosphate moiety of the phosphoribosyl pyrophosphate (PRPP), with production of nicotinamide mononucleotide (NMN) or nicotinate mononucleotide (NaMN) and pyrophosphate (PPi). Both classical niacin vitamins, Nam and Na, are physiologically relevant precursors for NAD; Nam is used in the amidated salvage route, whereas Na is used in the deamidated route, also known as the Preiss-Handler pathway (Magni et al., 2008). The two metabolic routes contribute to the overall NAD pool in mammals with different efficiency and in different combinations depending on the tissue (Mori et al., 2014), cell type (Zamporlini et al., 2014), and metabolic status (Ruggieri et al., 2015). In such metabolic context, NAMPT and NAPT are also recognized as rate-limiting (Hara et al., 2007; Revollo et al., 2004) and thus considered as key druggable targets (Galli et al., 2013; Magni et al., 2009).

Besides the PRTase reaction above, these two enzymes are known to catalyze a facultative ATP hydrolysis (ATPase). Most studies on this subject have been carried out on human NAMPT (Burgos et al., 2009; Burgos and Schramm, 2008), *Salmonella typhimurium* NAPT (Gross et al., 1996, 1998; Grubmeyer et al., 1999; Rajavel et al., 1998; Vinitsky and Grubmeyer, 1993), and human NAPT (Galassi et al., 2012). Such ATPase activity is intriguing since it couples weakly, i.e., not stoichiometrically, to the PRTase and involves the formation of a phosphor-His intermediate at the active site (phosphorylated H247 in human/murine NAMPT, H219 in *S. typhimurium* NAPT, and H213 in human NAPT). Therefore, NAMPT and NAPT are uniquely ATP-sensitive enzymes that have mechanistically evolved to regulate their own NMN/NaMN synthesis by linkage to an ATP-dependent autophosphorylation process. This link, however, is not mandatory and both enzymes readily synthesize pyridine mononucleotides even in the absence of ATP, albeit with decreased catalytic efficiency (Burgos and Schramm, 2008; Vinitsky and Grubmeyer, 1993). At physiological Mg^{2+}-ATP concentrations, NAMPT and NAPT are probably phosphorylated, providing efficient capturing of the pyridine substrate and conversion to the corresponding product. Thus, their ATPase activity is seen as an in vivo thermodynamic drive toward NMN/NaMN synthesis and, in this view, intracellular ATP is the fuel that, via these enzymes, allows recycling to NAD of the two niacin moieties even at very low intracellular concentration (Burgos and Schramm, 2008; Gross et al., 1998).

The complexity is further increased by the functional pleiotropism of NAMPT within mammalian organisms. Besides regulating

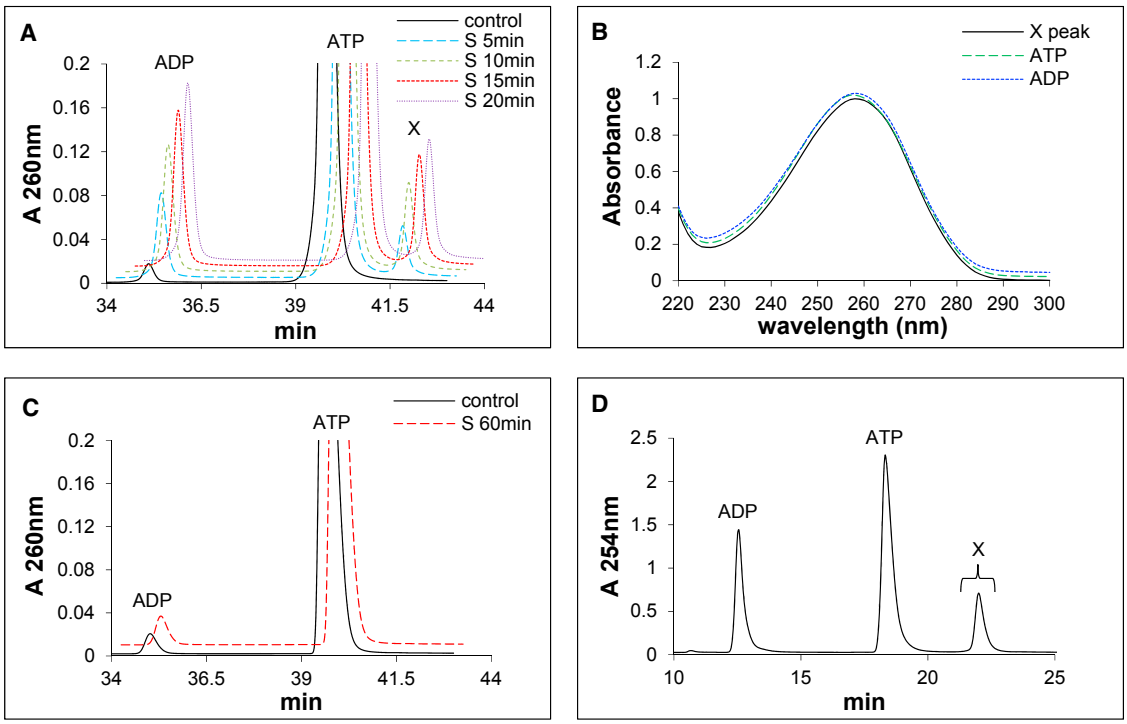

Figure 1. Identification of Ap4 as a New Enzymatic Product

(A) Analytical C18-HPLC UV profiles from a typical ATPase activity assay ("S") of murine NAMPT wild-type (~15 μM) incubated in the presence of 2.4 mM ATP. The horizontal axis shows only the region that visualizes the result. "X" indicates the newly identified reaction product. The "control" refers to a parallel blank mixture without the enzyme showing no hydrolysis of ATP and its negligible contamination by ADP.

(B) UV spectra of the peaks in (A), at comparable maxima corresponding to 1 absorbance unit.

(C) Analytical C18-HPLC UV profiles from a reaction assay carried out as in (A) but using the murine NAMPT mutant H247E (~40 μM).

(D) Preparative HPLC purification by TSK-DEAE chromatography of the enzymatically formed species X (the fractions collected are within the curly bracket).

intracellular NAD homeostasis (Revollo et al., 2004), NAMPT is subject to a circadian transcriptional control by the CLOCK machinery (Ramsey et al., 2009), it belongs to systemic regulatory networks (Rehan et al., 2014; Yoon et al., 2015), and it is a serum-circulating secreted protein known as PBEF (Samal et al., 1994) or visfatin (Fukuhara et al., 2005), which has an additional property as an immunomodulating cytokine (Audrito et al., 2015; Skokowa et al., 2009; Sun et al., 2013). Recently, the TLR4 receptor in human lung, which mediates the innate immunity response, has been identified as the receptor of circulating NAMPT (Camp et al., 2015), but controversies remain regarding the secretion mechanism of the enzyme, the involvement of NAMPT catalytic activity in the cytokine function (Li et al., 2008), and the bioavailability of enzyme reactants in extracellular fluids (Hara et al., 2011). As to NAPT, no extracellular function has been yet ascribed to this protein, but its presence in human sera as a circulating active enzyme has been recently reported (Zamporlini et al., 2014).

This work started from the serendipitous finding of an unpredicted reaction product formed in vitro by NAMPT and NAPT from the ATP substrate. We identified this product as adenosine 5′-tetraphosphate (Ap4) and proved it to be enzymatically formed by a phosphor-transfer reaction to ATP, i.e., an unforeseen additional reaction catalyzed by such type II PRTases. Ap4 is known as the most potent vasoactive purinergic mediator in mammals, circulating in plasma at nanomolar concentrations, and exerting vasoconstriction through activation of the P2X1 receptor (Tolle et al., 2008). Thus, the ability to synthesize Ap4 could be important for the extracellular signaling roles of these enzymes. Moreover, as Ap4 has long been known in mammals as an intracellular molecule of unclear metabolic origin (Fraga and Fontes, 2011), our data identify two of the enzymes likely to contribute to its homeostasis.

RESULTS

Ap4 Is an Authentic ATP-Derived Product of the NAMPT-Catalyzed Reaction

Initial C18-HPLC assays aiming to evaluate ATP usage by murine NAMPT showed the time-dependent formation of an unpredicted product in the reaction mixture, distinct from ADP (Figure 1A). Its UV spectrum was typical of an adenylate compound, i.e., superimposable to that of both ATP and ADP (Figure 1B). The unknown product was absent in control mixtures including heat-inactivated enzyme, or missing individual mixture components ATP and Mg^{2+} ions (not shown). Furthermore, the H247E mutant (Wang et al., 2006), which is ATP insensitive despite its retained NMN synthesis capability (Table 1), did not form any of this product (Figure 1C). This ruled out any non-enzymatic origin and suggested that it was a novel ATP-derived product of NAMPT.

The novel product was purified by TSK-DEAE chromatography for further characterization (Figure 1D). The purified

Table 1. PRTase and ATPase Activities by Orthologous NAMPT and NAPT Enzymes

Enzyme Species	Treatment	PRTase Rates (mU/mg)[a]		ATPase Rates (mU/mg)[b]			
		NMN Synthesis	NaMN Synthesis	ATP Consumption	ADP Synthesis	Pi Synthesis	Ap4 Synthesis
Murine NAMPT wild-type	none	31.1 (4.77)	5.86 (0.59)	8.54 (1.02)	5.82 (1.08)	3.19 (1.40)	2.66 (0.47)
	+FK866	ND	ND	10.4 (0.12)	9.58 (0.83)	9.02 (1.64)	1.51 (0.27)
Murine NAMPT H247E	none	3.21 (0.20)	ND	ND	≤0.02	≤0.02	ND
	+FK866	ND	ND	ND	≤0.02	≤0.03	ND
Human NAPT wild-type	none	ND	16.0 (1.15)	1.48 (0.08)	1.17 (0.10)	1.14 (0.21)	0.16 (0.04)
	+FK866	ND	15.5 (0.88)	1.57 (0.07)	1.25 (0.04)	1.31 (0.03)	0.19 (0.03)
Human NAPT H213A	none	ND	76.4 (11.2)	≤0.10	≤0.10	≤0.10	ND
	+FK866	ND	81.1 (3.82)	≤0.10	≤0.10	≤0.10	ND
Acinetobacter NadV wild-type	none	30.6 (1.84)	ND	1.14 (0.09)	1.01 (0.08)	0.89 (0.08)	0.12 (0.02)
	+FK866	8.04 (2.06)	ND	23.4 (2.96)	14.9 (1.22)	6.17 (1.65)	8.54 (2.06)
Staphylococcus PncB wild-type	none	ND	441 (56.7)	13.0 (0.39)	8.54 (0.25)	4.06 (0.11)	4.48 (0.14)
	+FK866	ND	424 (47.0)	14.3 (0.59)	9.38 (0.37)	4.44 (0.16)	4.94 (0.21)

Pure recombinant enzymes were used in these assays (see Figures S3 and S4; Tables S1 and S2). Data are represented as the mean and SD (in parentheses) from n = 3 experiments. ND, below the detection limit. FK866 was added in the indicated assays at a 50 μM final concentration.
[a]Rates measured at 0.5 mM concentration of each PRTase substrate, in the presence of 1 mM ATP.
[b]Rates measured at 2 mM concentration of ATP.

species was lyophilized to remove the volatiles, and resuspended in suitable solutions at concentrations that were calculated spectrophotometrically based on the adenosine content (see STAR Methods section). The solubilized species was found to be stable through several freezing/thawing cycles, and was next subjected to chemical, enzymatic, and liquid chromatography-electrospray ionization mass spectrometry (LC-ESI-MS) analyses. We identified a phosphate/adenosine stoichiometry of 4:1 (Figure 2A), a progressive digestion by alkaline phosphatase to ATP, ADP, AMP, and adenosine in this order (Figure 2B), digestion by phosphodiesterase to AMP and then to adenosine (Figure 2C), and a mass spectrum under the X peak of m/z 586 $[M-H]^-$ (Figure 2D). Orthogonal analysis of these results identified the purified NAMPT product as Ap4. Parallel enzyme digestion tests of a pure Ap4 standard yielded results identical to those obtained with the purified NAMPT product (Figure S1). Moreover, the NAMPT product and the Ap4 standard co-eluted after chromatography in two distinct separations, i.e., ion-pair reverse phase (Figure 2E) and anion exchange (Figure 2F). Taken together, this evidence indicates the novel NAMPT product is indeed an authentic Ap4 (Figure 3A).

Mechanism of the Enzymatic Formation of Ap4

Having identified the new Ap4 product, we carried out a quantitative time course analysis of the whole NAMPT-catalyzed ATPase reaction. Focusing on initial rates (Figure 4A, inset), we could observe: (1) a linear decline of the ATP substrate quantitatively matching the sum of the two adenylate products formed, i.e., ADP and Ap4; and (2) a linear rise of the other product, Pi, quantitatively matching neither ADP nor Ap4 alone but their difference. Hence, since a 1:1 stoichiometry between ADP and Pi is expected from ATP hydrolysis, these results indicated that, parallel to the hydrolysis of ATP to ADP and Pi, an additional reaction occurred whereby Pi reacted with ATP, leading to Ap4 formation. Thus, ATP was a substrate of two concomitant reactions generating both ADP and either Pi or Ap4. Moreover, by prolonging the incubation until ~75% of ATP was consumed (Figure 4A), we could observe a continuous, linear formation of Pi, whereas Ap4 accumulated transiently, as predicted from the reversibility of the reaction yielding its formation. The reversibility was also confirmed by direct assay of Ap4 as substrate (Figure S2A). Hence, accompanying a typically irreversible hydrolysis of ATP to ADP and Pi, is a fully reversible Pi transfer reaction between ATP and Ap4. Finally, we tested again under similar conditions the murine H247E NAMPT species, bearing a mutation on the His residue that becomes transiently phosphorylated during catalysis (Burgos et al., 2009; Wang et al., 2006). The negligible activity of this single-residue mutant (Figure 4B) confirmed that Ap4 synthesis by the wild-type enzyme is strictly associated to ATP hydrolysis and to the E-P intermediate formation. Notably, comparable results supporting the same conclusions were obtained from time course experiments performed with human NAPT (Figures S2B and S2D) and its H213A mutant (Figure S2E).

Together these lines of evidence strongly suggest a reaction mechanism illustrated in Figure 3B that stems from the known model for NAMPT and NAPT (Burgos et al., 2009; Rajavel et al., 1998), whereby a phospho-enzyme intermediate arises from ATP cleavage and subsequent ADP release (top half of Figure 3B). The phosphorylation back to ATP of the ADP product was previously demonstrated by isotope exchange experiments on both NAMPT (Burgos and Schramm, 2008) and NAPT (Honjo et al., 1966; Kosaka et al., 1971). We now add to the model the possibility that the enzyme-linked phosphoryl group can also be reversibly transferred to another molecule of ATP, thus generating Ap4 (bottom half of Figure 3B). By implication, the facultative ATPase activity of these enzymes serves not only hydrolysis fates but also a functional phosphor-transfer reaction that occurs via the same E-P intermediate to form Ap4. Of note, the ATP hydrolysis and phosphor-transfer reactions occur

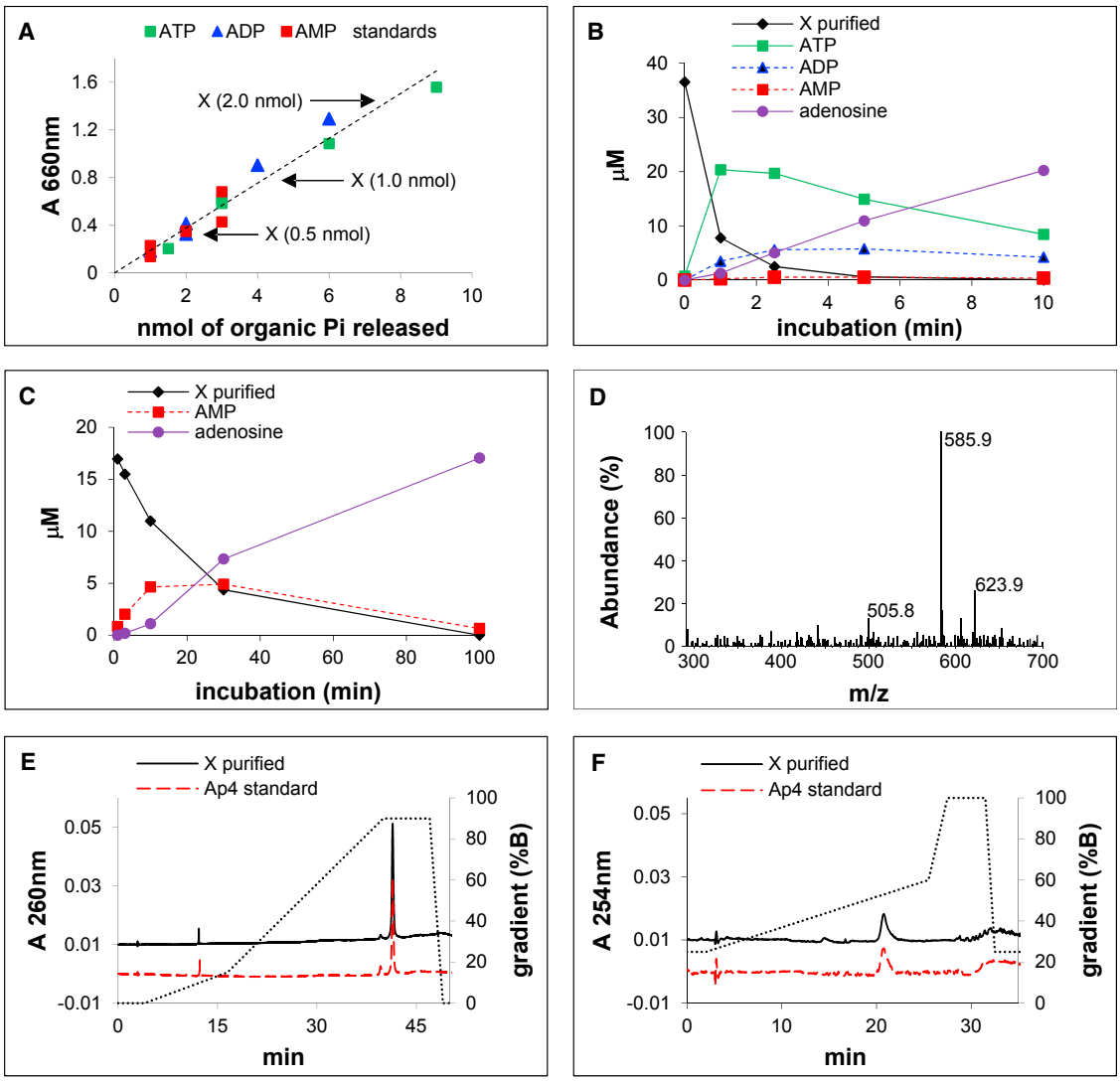

Figure 2. Structural Assessment of the Enzyme-Formed Ap4 Product

(A) Molar ratio in the purified species X between the organic phosphate released after chemical digestion and quantified by malachite green, and the adenosine content quantified by UV absorption (arrows). A reference curve was created from the indicated standards, all with known Pi/adenosine stoichiometry.

(B) Time course digestion of the purified species X by calf intestine alkaline phosphatase (see also Figure S1A).

(C) Time course digestion of the purified species X by snake venom phosphodiesterase I (including a contaminating 5′-nucleotidase that causes AMP-to-adenosine conversion, see also Figure S1B).

(D) LC-ESI-MS analysis of the purified species X.

(E) Analytical C18-HPLC UV profiles of the purified species X and an Ap4 standard (both ~0.8 nmol). Dotted line, the methanol gradient applied for elution.

(F) Analytical TSK-DEAE-HPLC UV profiles of the purified species X and an Ap4 standard (both ~0.8 nmol). Dotted line, the salt gradient applied for elution.

concomitantly but are dissectable, and individually measurable, by monitoring Pi and Ap4, respectively. Quantification of the released ADP provides instead an overall measure of their sum.

ATP Hydrolysis and Phosphor Transfer by Evolutionary Distant Type II PRTases

To assess whether the capability to form Ap4 is a distinctive feature among orthologous type II PRTases, we next characterized the catalytic properties of a bacterial NAMPT, i.e., the *nadV* gene product from *Acinetobacter baylyi*, as well as of a bacterial counterpart of human NAPT, i.e., the *pncB* gene product from *Staphylococcus aureus*. Analysis was also performed on the aforementioned mutants of murine NAMPT and human NAPT, both missing the phosphorylatable His residue at their catalytic site. Information about cloning, structure, and the bacterial expression of these recombinant proteins is given in the Supplemental Information (Table S1; Figures S3 and S4).

First, PRTase activities were measured at fixed millimolar concentrations of substrates (PRPP and either Nam or Na), in the presence or absence of micromolar concentrations of FK866, the best-characterized selective inhibitor of NAMPT (Colombano et al., 2010; Galli et al., 2013). These assays were carried out in

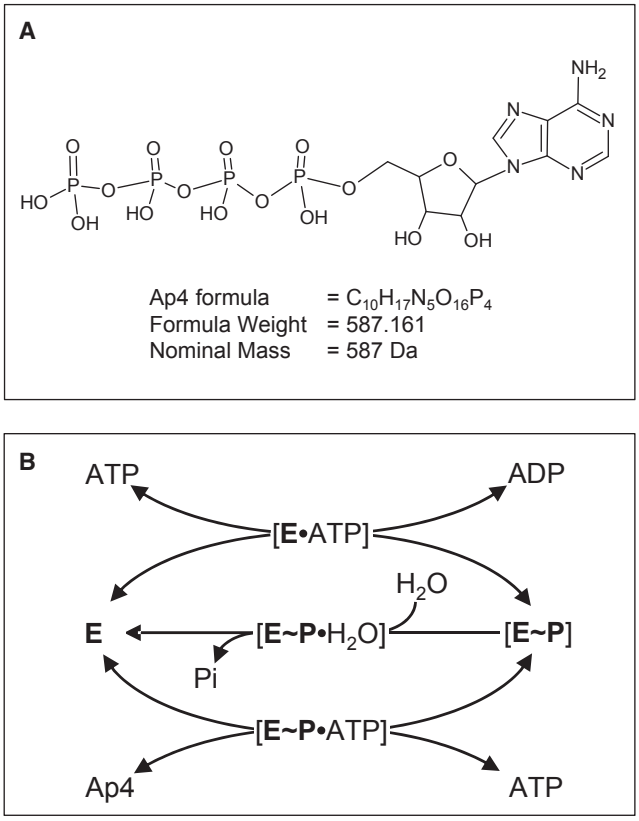

Figure 3. The Ap4 Structure and Mechanism for Enzymatic Synthesis and Degradation

(A) Chemical structure and properties of Ap4.

(B) Kinetic scheme for the branched-mechanism hydrolysis/transferase reactions operated by NAMPTs and NAPTs on the ATP substrate.

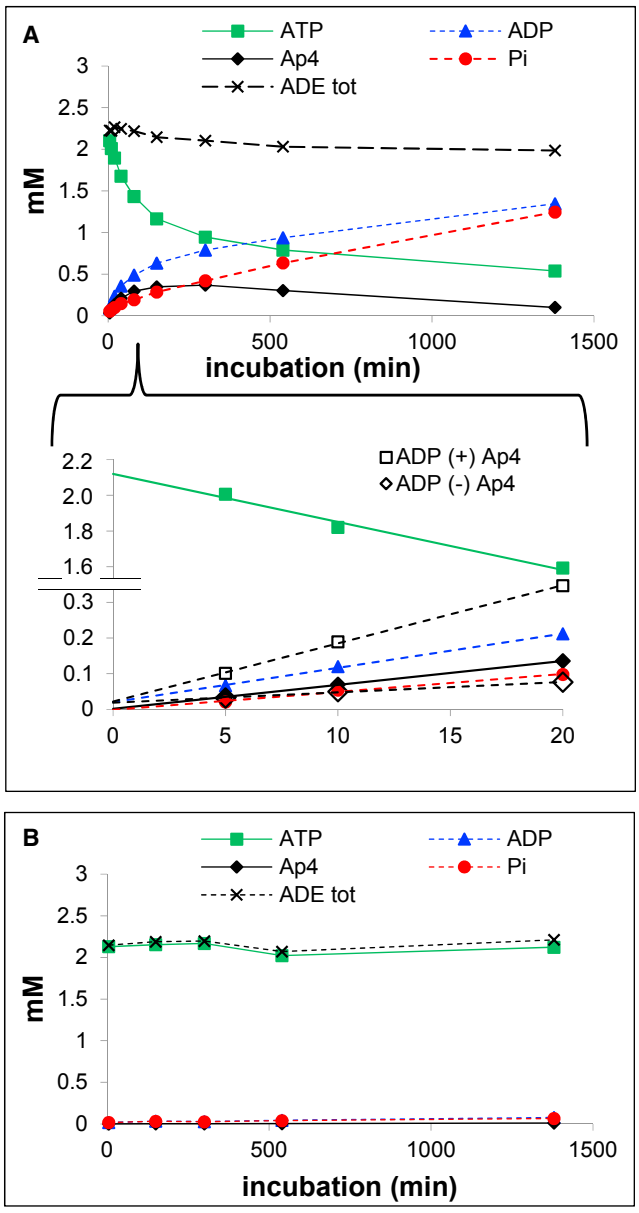

Figure 4. Time Course Analysis of the ATPase Reaction Catalyzed by Murine NAMPT

(A) Quantitative time course analysis of the ADP, Ap4, and Pi products formed by murine NAMPT wild-type (~35.5 μM) after incubation in the presence of 2 mM ATP (see also Figure S2C). ADE tot refers to the sum of adenylate compounds at each time. Bottom inset, initial incubation (first 20 min) in an expanded scale, also showing the sum and the difference of ADP- and Ap4-formed products. Data from C18-HPLC analysis and malachite green assays were subtracted by the respective backgrounds evaluated in parallel control assays carried out without enzyme. Not shown, ATP re-addition after 24 hr incubation restored the original activity.

(B) Time course as in (A) but in the presence of the murine NAMPT mutant H247E (~21.6 μM).

the presence of ATP, once the ATP sensitivity of the PRTase reaction catalyzed by these enzymes was confirmed (Table S2). As detailed in Table 1, a selective pyridine substrate recognition by each NAMPT and NAPT tested was found, with the exception of a modest activity exhibited by murine NAMPT toward the Na substrate, as also reported by others (Khan et al., 2006). As expected, the PRTase activity of both murine and bacterial NAMPTs was inhibited by FK866, whereas all NAPTs were insensitive to the inhibitor. Subsequently, ATPase activities were assayed at fixed millimolar concentrations of ATP. Pi formation rates for the hydrolysis reaction and Ap4 formation rates for the phosphor-transfer reaction were measured. ADP formation and ATP consumption were also measured to verify the proportion with the two rates above (Table 1). As a result, both mutants tested were confirmed to be almost devoid of any ATPase activity, while all wild-type enzymes showed individual rates stoichiometrically consistent to each other as described above for murine NAMPT (Figure 4A), including an Ap4 formation in keeping with the proposed model (Figure 3B). This indicated that the mechanism of catalysis underlying ATP degradation is evolutionarily conserved in both NAMPT and NAPT from bacteria to mammals.

Unexpectedly, the ATPase activity of both NAMPTs tested was not blocked but rather stimulated in the presence of FK866. The activation was evident considering the ATP consumption and Pi synthesis rates (Table 1). Focusing instead on Ap4 synthesis, the rate was slightly reduced in the presence of FK866 in murine NAMPT and highly increased (~70-fold) in the

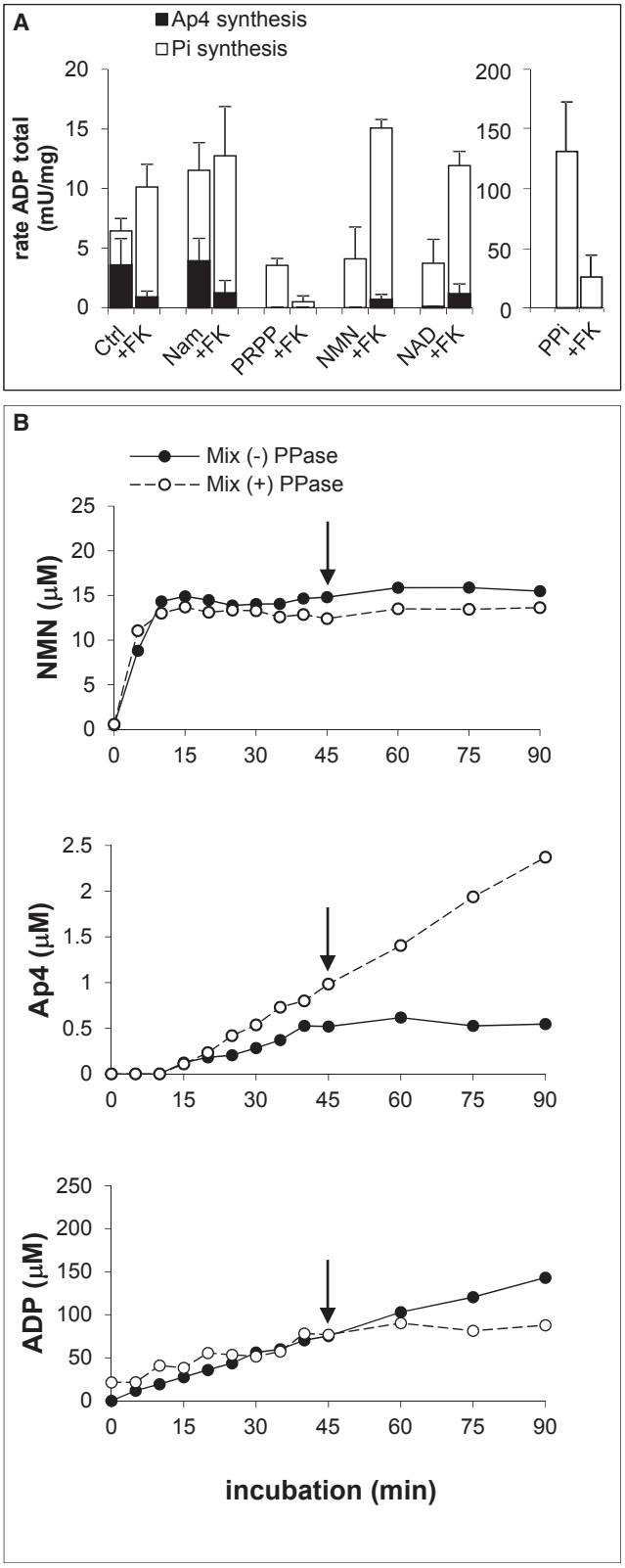

Figure 5. In Vitro Assays of Murine NAMPT ATPase versus PRTase Activities

(A) ATP hydrolysis (white bars) and phosphor-transfer (black bars) rates catalyzed by murine NAMPT wild-type (~5.2 μM in the assay) in the presence of 2 mM ATP and 0.5 mM of either NAD or each PRTase reactant as indicated. "Ctrl" represents the control carried out in the absence of any compound above but ATP. "+FK" refers to parallel assays where the enzyme was pre-incubated with FK866 (50 μM final) before addition of any other compound. Reactions were started by addition of ATP. On the right, in an expanded y axis, a separate graph for PPi is presented in order to visualize the results. Values represent the mean + SD from a triplicate assay.

(B) Time course analysis of the reaction catalyzed by murine NAMPT (0.52 μM in the assay) in the presence of 2 mM ATP, 0.5 mM Nam, and 0.02 mM PRPP. The assay was duplicated with PPase ~100 mU/mL (~20-fold excess with respect to the measured ATP-coupled PRTase activity rate of NAMPT). Reactions started by addition of all substrates at once, i.e., by using a pre-mixed solution of ATP, Nam, and PRPP. Arrows indicate the reaction time where 50 μM FK866 was added. The accumulating products NMN (upper panel), Ap4 (middle panel), and ADP (bottom panel), were individually quantified after ion-pair C18-HPLC analysis, and their concentration in the reaction mixture indicated. The HPLC data of ADP were corrected by subtracting the contaminating background present in the stock ATP solution used.

bacterial NAMPT (Table 1). These data surprisingly showed that FK866 may elicit the facultative reaction leading to Ap4 synthesis in both mammalian and bacterial NAMPTs, in contrast to the strong inhibition exhibited toward their intrinsic activity leading to NMN synthesis.

In Vitro Modulation of Murine NAMPT ATPase versus PRTase Activities

We then investigated the ATPase and PRTase reactions simultaneously, as would be expected in a physiological setting. Initially, we set the ATPase assays of murine NAMPT in the presence of each individual PRTase reactant (Figure 5A). We also tested the effect of known modulators including NAD, given its reported feedback-regulatory inhibition on PRTase (Burgos and Schramm, 2008), and FK866, given the above-observed inhibition on PRTase but not ATPase (Table 1). While FK866 is known to inhibit both the ATP-coupled and the ATP-uncoupled PRTase reactions, NAD appears effective only toward the ATP-coupled reaction (Burgos and Schramm, 2008), thus suggesting a differential regulation on the ATPase activity.

In substantial agreement with the properties described for human NAMPT (Burgos and Schramm, 2008), ADP formation was stimulated by PPi and Nam, but inhibited by PRPP, NMN, and NAD (Figure 5A). In more detail, ATP hydrolysis was highly stimulated by PPi and, to a lower extent, by Nam, while Ap4 formation was remarkably inhibited by all tested metabolites with the exception of Nam, which showed no effect (Figure 5A). The presence of FK866 in the reaction mixtures tended to enhance the effects of Nam and PRPP, and to counteract those of PPi and NMN. Intriguingly, the dinucleotide NAD fully mimicked the effect of its mononucleotide NMN, in both the presence and absence of FK866 (Figure 5A).

These data broadly indicated that NAMPT ATPase and its Ap4 synthesis may be finely regulated by compounds that bind the enzyme active site in different manners (Burgos et al., 2009; Khan et al., 2006; Wang et al., 2006), resulting in either synergistic or antagonistic effects, depending on the case. In addition, they suggest how the enzyme-mediated Ap4 synthesis could be regulated in mammalian cells. Indeed, given that NMN and PPi are present at low steady-state levels (Mori et al., 2014), and hence their effect on Ap4 synthesis might be negligible, it appears that, alongside NAD, PRPP may be another primary

Table 2. Adenylate and Pyridine Compounds in Melanoma B16 Cells

nmol/mg of Protein

B16 Cells	Ap4	ATP	ADP	Nam	NMN	NAD
WT (n = 9)	0.527 (0.068)	9.107 (1.595)	8.992 (2.056)	4.344 (0.721)	0.039 (0.007)	4.489 (1.524)
WT +FK866 (n = 7)	0.923 (0.101)**	5.882 (0.605)	7.654 (1.385)	3.056 (0.535)	0.010 (0.002)*	Nd
FLAG-NAMPT (n = 3)	1.073 (0.175)**	17.22 (0.546)	13.32 (0.454)	2.417 (0.097)	0.212 (0.068)***	6.940 (0.122)
shNAMPT low (n = 5)	0.329 (0.075)^{ns}	5.347 (1.027)	5.972 (1.125)	3.281 (0.311)	0.026 (0.005)^{ns}	2.135 (0.289)

B16 cells with modulated intracellular expression of NAMPT (see Figure S5), or treated with 100 nM FK866 for 24 hr, were collected and evaluated for their nucleotides levels by LC-ESI-MS analysis. WT, wild-type cells. shNAMPT low, cells engineered for NAMPT silencing. FLAG-NAMPT, cells engineered for NAMPT overexpression. Data are represented as the mean and SEM (in parentheses) from n experiments, as indicated. Statistical analysis for Ap4 values: p = 0.09 (ns) for shNAMPT low vs WT cells; p = 0.0048 (**) for FLAG-NAMPT vs WT cells; p = 0.0047 (**) for WT + FK866 vs WT cells. Statistical analysis for NMN values: p = 0.19 (ns) for shNAMPT low cells vs WT cells; p = 0.0009 (***) for FLAG-NAMPT vs WT cells; p = 0.045 (*) for WT +FK866 vs WT cells. Nd, below the detection limit.

negative regulator of NAMPT under normal conditions. To corroborate this, we assayed the ATP-coupled PRTase reaction at a PRPP concentration saturating for the enzyme (Burgos and Schramm, 2008), but ~25-fold lower than that of the other substrate Nam (Figure 5B), and evaluated the formation of Ap4 under these conditions. The assay was duplicated in the presence of inorganic PPase in order to prevent accumulation of the PPi product, and in both mixtures FK866 was added after ~45 min incubation, as depicted in Figure 5B (arrow). As described above, Ap4 formation represents the phosphor-transfer reaction, while ADP formation accounts for both phosphor-transfer and hydrolysis reactions. Both time course analyses showed a linear initial synthesis of NMN until PRPP was almost totally consumed (Figure 5B upper). In this early phase, we could measure ADP formation (Figure 5B bottom), but no production of Ap4 (Figure 5B middle). However, soon after the PRTase reaction reached near equilibrium as indicated by the observed NMN plateau, the Ap4 product started to be formed and its synthesis increased linearly over time (Figure 5B middle). Addition of FK866 during Ap4 synthesis resulted in distinct effects on the PPase-treated versus the PPase-untreated reaction; while in the former the synthesis of Ap4 continued, in the latter it was blocked (Figure 5B, middle). This contrasts with ADP formation after FK866 addition (Figure 5B, bottom). Overall, these in vitro results suggested (1) a physiologically feasible NAMPT-mediated Ap4 synthesis under the naturally low, fluctuating concentrations of most endogenous PRTase reactants, (2) the possibility of fine-tuning and dissecting NMN and Ap4 formation, and (3) a likely pharmacological regulation by FK866.

In Vivo Regulation of Ap4 Levels by NAMPT in Murine Cells and Plasma

We then proceeded to evaluate Ap4 levels in mammalian cells and their dependence on NAMPT in vivo. For this we used an in-house B16 melanoma cell line previously shown to be enriched in NAMPT (Maldi et al., 2013). We had previously engineered (Grolla et al., 2015) an overexpressing cell line (B16 FLAG-NAMPT) expressing ca. 160% of wild-type NAMPT levels, and a silenced cell line (B16 shNAMPT Low) expressing less than 20% of wild-type NAMPT (see Figure S5 for expression levels). The levels of the nucleotides of interest determined by LC-ESI-MS in these cells are reported in Table 2. The overall data show a low ATP/ADP ratio that has also been observed by others (Huang et al., 2003) in the same cell type (B16), as well as higher than expected Nam levels, which can be explained by the presence of high micromolar concentrations of Nam in the commercially available medium in which cells were grown (32.7 μM, as depicted in the product datasheet). It is unlikely that the low ATP/ADP ratio, as well as the high Nam/NAD ratio, are instead given by degradation during sample preparation, as standards were processed in parallel with no sign of degradation. As expected, NMN and NAD levels correlated with NAMPT expression. More surprisingly, the Nam levels were lower in shNAMPT compared with wild-type NAMPT. Notably, we could measure intracellular Ap4 levels at 0.527 ± 0.068 nmol/mg. Such levels were increased in cells overexpressing NAMPT, and reduced in cells silenced for the enzyme. We also observed an almost doubling of the Ap4 content in wild-type cells treated with FK866 (Table 2). Such doubling was accompanied by the depletion of NMN and NAD, as expected, and by a marked reduction of Nam. These data, taken together, suggest that NAMPT is a source of intracellular Ap4, although we cannot rule out the possibility that other enzymes also contribute. The effect observed in the presence of FK866 could in part be explained by the uncoupling of the two reactions, as shown by the experiments performed on the purified enzymes, and in part could suggest that a cellular homeostatic control is present.

Ap4 levels under conditions of metabolic perturbation were also evaluated. We assayed Ap4 levels in cells grown for 20 hr in serum-free conditions, in low-glucose conditions (normal concentration of 4.5 g/L to a low concentration of 1 g/L), and in both low-glucose and serum-free conditions. Levels of Ap4 were reduced in all three conditions, but were statistically reduced only when cells were grown in low concentration of glucose (Figure 6A). On the contrary, NMN levels were statistically reduced only when cells were grown in the absence of serum (Figure 6B). Treating cells with H_2O_2 (500 μM) reduced both Ap4 and NMN levels, but this change was not statistically significant.

Furthermore, given the extracellular role of secreted NAMPT, we decided to explore whether we could detect Ap4 in murine plasma and whether circulating NAMPT levels correlated with plasma Ap4 levels. To this end, we sampled blood from mice for both NAMPT (via an ELISA assay) and Ap4 levels (by LC-ESI-MS). In most samples Ap4 was detectable with a global mean of 562 ± 114 nM (n = 23). This is similar to a previous report of Ap4 in human plasma at 255.6 ± 82.4 nM (Tolle et al., 2008). In

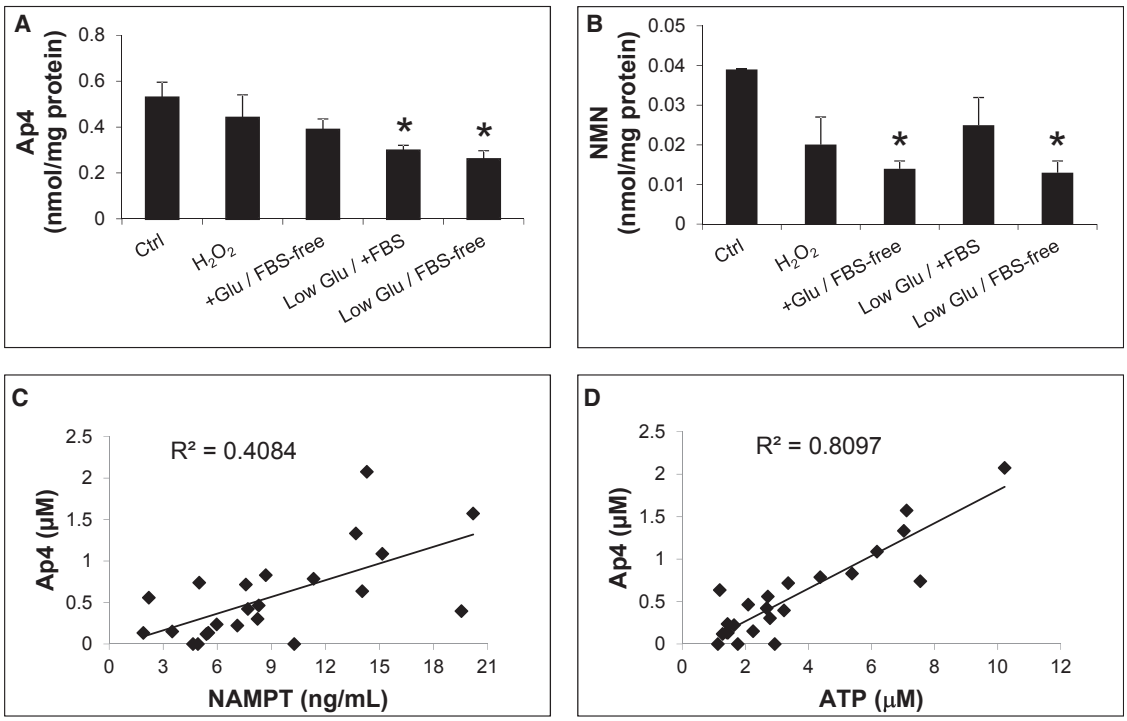

Figure 6. In Vivo Nucleotide Levels in Mouse Cultured Cells and Plasma

(A and B) Ap4 (A) and NMN (B) levels evaluated by LC-ESI-MS in B16 wild-type cells under metabolism perturbations obtained by growth for 20 hr in serum (fetal bovine serum [FBS])-free conditions, in low-glucose (Low Glu) conditions (from 4.5 to 1.0 g/L), in both low-glucose and serum-free conditions, or treatment with 500 μM H_2O_2. *p = 0.05 for Ap4 levels of B16 in Low Glu/+FBS condition versus ctrl cells; *p = 0.029 for Ap4 levels of B16 in Low Glu/FBS-free condition versus ctrl cells; *p = 0.03 for NMN levels of B16 in +Glu/FBS-free condition versus ctrl cells; *p = 0.05 for NMN levels of B16 in Low Glu/FBS-free condition versus ctrl cells. Values represent the mean + SEM from a triplicate assay.

(C and D) The Ap4 levels measured by LC-ESI-MS in the plasma of healthy male C57BL/6 mice (n = 23 total analyzed samples) and their correlation with extracellular NAMPT (C) and ATP (D). The linear regression value (R^2) is highlighted.

addition, these Ap4 levels, despite their inter- and intra-subject variability, showed a good correlation with extracellular NAMPT levels (Figure 6C, R^2 = 0.41). Not surprisingly, Ap4 also correlated, to a greater extent, with ATP levels measured in parallel (Figure 6D, R^2 = 0.81). These data are consistent with the notion that extracellular NAMPT may be one of the enzymes that participates in the synthesis of Ap4, and that Ap4 is derived enzymatically from ATP.

DISCUSSION

Ap4 was first described in the early 1950s as a contaminant of commercial ATP preparations (Marrian, 1954), and re-emerged in the literature about 50 years later as an extracellular vasoactive compound (Pintor et al., 2004; Tolle et al., 2008). It has a broad distribution in prokaryotes and eukaryotes, including mammalian tissues and plasma, and has been identified as an in vitro by-product of a number of ATP-dependent enzymatic reactions (see Fraga and Fontes, 2011, and the list of enzymes therein). Given the lack of any dedicated enzyme to its synthesis, Ap4 in vivo is thought to arise from the promiscuous activity of multiple enzymes, and no information about its physiological regulation is currently available. Yet, given that Ap4, at subnanomolar concentrations, is one of the most potent vasoconstrictors known to date (Tolle et al., 2008), and nanomolar concentrations of Ap4 can modulate the intraocular pressure in the rabbit eye (Pintor et al., 2004), it seems unlikely that its production would not be regulated. These actions of extracellular Ap4 are also mediated by P2X receptors (Pintor et al., 2004; Tolle et al., 2008) that belong to a structural family of membrane ion channels, with a widespread tissue distribution in mammals, where they underlie a variety of functions, including excitatory effects on smooth muscle cells (depolarization/contraction), Ca^{2+} uptake into neurons (neuromodulatory responses), and release of pro-inflammatory cytokines such as interleukin 1β from immune cells (North, 2016). On the other hand, intracellular functions of Ap4 are only putative at present but potentially relevant in fundamental biological processes like, for example, the cellular protein turnover, as suggested by the observed in vitro targeting of Ap4 to AMP-forming ligases, aminoacyl-tRNA synthetases (Retailleau et al., 2007), and the ubiquitin-activating enzyme E1 of the proteasome system (Gunther Sillero et al., 2005).

To our knowledge, the data presented here establish for the first time that two enzymes belonging to the class of type II PRTases, long thought to be committed to NAD synthesis in living cells with a non-obligatory accompanying use of ATP, are also capable of synthesizing Ap4 (Figure 3A). We propose a mechanism shared by NAMPT and NAPT, where the known ATP hydrolysis is coupled to a new phosphor-transfer reaction

that, via the same E-P complex intermediate, leads to Ap4 synthesis (Figure 3B). Notably, the facultative ATPase of both enzymes has been extensively studied in the past as a paradigm for energy use (Burgos and Schramm, 2008; Grubmeyer et al., 1999), but the reaction as such went partially unnoticed due to its cryptic nature and, most likely, to the lack of a stoichiometric evaluation of all reactants involved. Nevertheless, in support of our model, mechanisms similar to the proposed one apply to other enzymes forming covalent intermediates during their catalytic cycle. For example, glucose-6-phosphatase (Sukalski and Nordlie, 1989), transglutaminases (Chung and Folk, 1972), and nucleotidases (Amici et al., 2002) are all known to catalyze branched-pathway reactions characterized by double-displacement mechanisms and formation of covalently modified enzyme intermediates (phosphorylated or acylated) that preserve the transfer potential of the group undergoing transfer.

One peculiarity of NAMPT and NAPT is that such use of ATP may occur independently from NMN/NaMN synthesis, the intrinsically catalyzed reaction for which they were originally classified and that remains the focus of most current studies. Notably, only NAMPTs and NAPTs from both bacterial and mammalian sources are known to use ATP hydrolysis and to catalyze a dual PRTase reaction, whether ATP coupled or ATP uncoupled (Burgos and Schramm, 2008; Galassi et al., 2012; Gross et al., 1998; Sorci et al., 2010). The other classified PRTase members, including adenine (EC 2.4.2.7), hypoxanthine/guanine (EC 2.4.2.8), uracil (EC 2.4.2.9), orotate (EC 2.4.2.10), quinolinate (EC 2.4.2.19), and dioxotetrahydropyrimidine (EC 2.4.2.20) PRTases are widely considered to be ATP insensitive, albeit supporting experimental evidence exists in only a few cases (Gholson et al., 1964; Shimosaka et al., 1985). To confirm this, we have tested the ATP dependence of a bacterial quinolinate PRTase and a member of the hypoxanthine/guanine PRTase family. The results showed the ATP insensitivity of both these PRTases (Figures S4 and S6; Table S2). It should also be noted that quinolinate PRTase, the closest functional and structural relative of NAMPT and NAPT (Marletta et al., 2015), lacks the conserved His residue that is essential for Ap4 formation according to our scheme (Figure 3B) and catalyzes a reaction of irreversible nature due to a decarboxylation step occurring along with the phosphoribosyl transfer (Bello et al., 2010), so that there is no need of ATP hydrolysis to drive the reaction. On the contrary, in both NAMPT and NAPT, ATP is used to establish the formation of a phosphohistidine intermediate (Burgos et al., 2009; Gross et al., 1996) that has been shown to potentiate their PRTase activity (Burgos and Schramm, 2008; Vinitsky and Grubmeyer, 1993), thereby enhancing cellular NAD synthesis. Nonetheless, in both NAMPT and NAPT, the reaction coupling ATP hydrolysis to NMN/NaMN synthesis is not stoichiometric and only a small part of the energy released from the hydrolysis is efficiently captured (Burgos and Schramm, 2008; Gross et al., 1998). This appreciable thermodynamic leak suggests additional roles exerted by the facultative ATPase reaction, perhaps independent from coupling. In this regard, our finding that it may drive Ap4 synthesis is an intriguing explanation. This is also supported by the observed catalytic similarity between mammalian and bacterial orthologs (Table 1), which suggests an intrinsic role for the Ap4 synthesis mediated by these enzymes, fully conserved throughout evolution.

Focusing on murine NAMPT, whether as an intracellular enzyme acting in the amidated NAD-salvaging route (Mori et al., 2014) that chiefly regulates NAD homeostasis (Revollo et al., 2004) or as an extracellular cytokine (Li et al., 2008; Sun et al., 2013), we provide evidence for an Ap4 synthesis of potential relevance at both the cellular and systemic level. First, the NAMPT ATPase is modulated in vitro by several compounds targeting the enzyme active site, suggesting a capability to synthesize Ap4 from ATP both intracellularly, in the presence of PRTase reactants (Figure 5), and extracellularly, in the absence of most of them (Hara et al., 2011). Second, in vivo Ap4 levels correlate with intracellular and, to some extent, extracellular NAMPT expression levels (Table 2; Figure 6C), pointing that NAMPT may regulate Ap4 homeostasis in different mammalian tissues. Third, metabolic perturbation in cells is able to modulate both Ap4 and NMN synthesis, albeit to different extents (Figures 6A and 6B). Fourth, the treatment with FK866, a selective inhibitor of NAMPT PRTase, but not of NAMPT ATPase (Table 1), downregulates intracellular NAD levels (Khan et al., 2006; Magni et al., 2009), but in contrast it upregulates intracellular Ap4 levels (Table 2). This latter observation further indicates that the intrinsic and facultative reactions catalyzed by NAMPT should be equally considered when investigating the effects of NAMPT inhibitors.

Indeed, an additional finding from our work is that NAD and FK866 exert opposite effects on NAMPT regarding its Ap4 synthesis, respectively inhibiting or potentiating it. Both compounds target NAMPT at the active site but, while NAD competes with PRPP (Burgos and Schramm, 2008), FK866 binds at the dimer interface and competes with Nam for binding (Khan et al., 2006; Marletta et al., 2015). In keeping with such distinct binding sites, we observed that FK866 behaves like Nam in potentiating the ATPase activity, while NAD behaves like PRPP in preventing it (Figure 5A). This leads to suggest that FK866 binding to the catalytic pocket of NAMPT, contrary to NAD binding, does not block ATP binding and its catalytic processing. Furthermore, as reflected by the picomolar versus nanomolar K_i values reported for FK866 and NAD, respectively (Burgos and Schramm, 2008), we found that micromolar concentrations of FK866 can neutralize the effect of millimolar NAD in vitro (Figure 5A). Therefore, NAMPT targeting by FK866 results in a novel biological effect, i.e., the rise of physiological Ap4 levels, in addition to the well-documented NAD depletion effect. This should be taken into account when evaluating the actions of this drug.

From the point of view of cell physiology, the coincidental identification of Ap4 synthesis by NAMPT and NAPT might underlie a dual level regulation of NAD biosynthesis: a direct one, through the NMN/NaMN-forming activity, and an indirect one, through Ap4 signaling. In a plausible scenario, for example, Ap4 would reroute protein resources toward de novo NAD biosynthesis, which in mammals starts from tryptophan. Indeed, while inhibiting aminoacyl-tRNA synthetases (Retailleau et al., 2007), Ap4 might support the activity of proteasome (Gunther Sillero et al., 2005), both processes converging in boosting tryptophan bioavailability. Speculation on the possible involvement

of Ap4 in other intracellular pathways is hard to present at the moment, as the physiological targets for Ap4 are only putative. On the other hand, in an extracellular context, Ap4 has recognized functions on purinergic signaling. In the rabbit eye this established function might be related to local NAMPT (Pintor et al., 2004). Furthermore, our observation that ATP and Ap4 are both circulating in murine plasma, where NAMPT is also present (Figures 6C and 6D), confirms earlier reports (Hara et al., 2011; Tolle et al., 2008) and suggests the possibility that some extracellular functions of NAMPT might be based on its enzymatic synthesis of Ap4. In this light, it would be worth reassessing the reported cytokine-like functions of extracellular NAMPT (Grolla et al., 2015; Zhao et al., 2014). The debate about the existence of a link between the molecular action and the enzymatic function of extracellular NAMPT is not yet settled, and our results provide new important elements that should not be overlooked.

In conclusion, we have shown that NAMPT appears to be directly coupled to intracellular and/or extracellular Ap4 homeostasis in mammals. Given that both the intracellular and extracellular forms of this enzyme are recognized as relevant in a number of disease states (Garten et al., 2015; Grolla et al., 2016; Imai, 2009; Shackelford et al., 2013), and that Ap4 has been already recognized as a potent signaling molecule, future work on this enzyme should not disregard this novel function. Further investigation should also encompass the other NAD biosynthetic enzyme, NAPT, endowed with the same catalytic property.

SIGNIFICANCE

This study reports additional catalytic properties of NAMPT and NAPT, two ubiquitous enzymes that are crucial for the synthesis of the essential redox co-factor NAD. They share structural similarity and dual location in mammals, i.e., both intracellular and extracellular. Extracellular NAMPT is also regarded as a cytokine endowed with multiple signaling functions, and whether its catalyzed reaction is pertinent to these actions is at present unclear, with contradictory evidence from different experimental settings. From a catalytic point of view, both NAMPT and NAPT appear profligate consumers of ATP. Indeed, they use a facultative ATP hydrolysis to promote their NAD biosynthesis activity by weak energy coupling. This paradigmatic reaction represents the main subject of our investigation. Our most significant finding is that bacterial and mammalian NAMPTs and NAPTs can also use ATP to form adenosine 5′-tetraphosphate (Ap4), a prominent signaling molecule of an as-yet unclear biochemical origin. Based on in vitro and in vivo evidence, we propose (1) a mechanism for Ap4 synthesis, (2) a chief contribution of NAMPT to Ap4 homeostasis in mammals, and (3) a reassessment of the NAMPT drug targeting in this light. Indeed, we demonstrate that in vivo targeting of NAMPT by FK866, a drug inhibitor of NAD synthesis, results in a parallel upregulation of Ap4 levels. This opens up pharmacological scenarios possibly missed before. In a broader perspective, a direct link of NAMPT to Ap4 formation suggests novel mechanisms by which this enzyme, intracellularly and extracellularly, may exert the plethora of actions that are attributed to it.

STAR★METHODS

Detailed methods are provided in the online version of this paper and include the following:

- KEY RESOURCES TABLE
- CONTACT FOR REAGENT AND RESOURCE SHARING
- EXPERIMENTAL MODEL AND SUBJECT DETAILS
  - Cell Lines
  - Animals
- METHOD DETAILS
  - Preparative HPLC Chromatography
  - Chemical and Enzymatic Digestion of the Purified NAMPT Product
  - Cloning, Expression, and Purification
  - Activity Assays
  - Cell Extraction for Western Blot Analysis
  - Cell Extraction for MS Analysis
  - Mouse Plasma Sampling and Treatment
  - LC-ESI-MS analysis of Pyridine and Adenine Nucleotides
- QUANTIFICATION AND STATISTICAL ANALYSIS

SUPPLEMENTAL INFORMATION

Supplemental Information includes six figures and two tables and can be found with this article online at http://dx.doi.org/10.1016/j.chembiol.2017.03.010.

AUTHOR CONTRIBUTIONS

Conceptualization, A.A. and G.O.; Methodology, A.A., A. Grolla, E.D.G., A. Genazzani, and G.O.; Investigation, A.A., A. Grolla, C.T., S.G., M.B., R.B., and G.O.; Resources, A.A., A. Grolla, E.D.G., L.S.; Writing – Original Draft, G.O.; Writing – Review & Editing, L.S., N.R., A. Genazzani, and G.O.; Funding Acquisition, A.A., A. Genazzani, N.R, S.R., and G.O.; Supervision, S.R., A. Genazzani, and G.O.

ACKNOWLEDGMENTS

This work was funded by grants RSA 2011-13 & 2012-14, Polytechnic University of the Marche (A.A., N.R., S.R., and G.O.) and by grants Associazione Italiana per la Ricerca sul Cancro (AIRC: IG10509) and Fondazione San Paolo (A. Genazzani). The authors thank Prof. Michael Coleman (University of Cambridge, UK) for critical reading of the manuscript, Nausicaa Clemente (Università del Piemonte Orientale, Novara, Italy) for technical support in breeding and housing of laboratory mice, Dr. Ubaldina Galli (Università del Piemonte Orientale, Novara, Italy) for generous providing of in-house synthesized FK866, and Dr. Francesca Mazzola (Polytechnic University of Marche, Ancona, Italy) for help in purification of *S. pyogenes* quinolinate PRTase.

Received: October 5, 2016
Revised: February 3, 2017
Accepted: March 14, 2017
Published: April 13, 2017

REFERENCES

Amici, A., Emanuelli, M., Ruggieri, S., Raffaelli, N., and Magni, G. (2002). Kinetic evidence for covalent phosphoryl-enzyme intermediate in phosphotransferase activity of human red cell pyrimidine nucleotidases. Methods Enzymol. *354*, 149–159.

Audrito, V., Serra, S., Brusa, D., Mazzola, F., Arruga, F., Vaisitti, T., Coscia, M., Maffei, R., Rossi, D., Wang, T., et al. (2015). Extracellular nicotinamide

phosphoribosyltransferase (NAMPT) promotes M2 macrophage polarization in chronic lymphocytic leukemia. Blood *125*, 111–123.

Balducci, E., Emanuelli, M., Raffaelli, N., Ruggieri, S., Amici, A., Magni, G., Orsomando, G., Polzonetti, V., and Natalini, P. (1995). Assay methods for nicotinamide mononucleotide adenylyltransferase of wide applicability. Anal. Biochem. *228*, 64–68.

Bello, Z., Stitt, B., and Grubmeyer, C. (2010). Interactions at the 2 and 5 positions of 5-phosphoribosyl pyrophosphate are essential in *Salmonella typhimurium* quinolinate phosphoribosyltransferase. Biochemistry *49*, 1377–1387.

Burgos, E.S., and Schramm, V.L. (2008). Weak coupling of ATP hydrolysis to the chemical equilibrium of human nicotinamide phosphoribosyltransferase. Biochemistry *47*, 11086–11096.

Burgos, E.S., Ho, M.C., Almo, S.C., and Schramm, V.L. (2009). A phosphoenzyme mimic, overlapping catalytic sites and reaction coordinate motion for human NAMPT. Proc. Natl. Acad. Sci. USA *106*, 13748–13753.

Camp, S.M., Ceco, E., Evenoski, C.L., Danilov, S.M., Zhou, T., Chiang, E.T., Moreno-Vinasco, L., Mapes, B., Zhao, J., Gursoy, G., et al. (2015). Unique toll-like receptor 4 activation by NAMPT/PBEF induces NFkappaB signaling and inflammatory lung injury. Sci. Rep. *5*, 13135.

Chung, S.I., and Folk, J.E. (1972). Kinetic studies with transglutaminases. The human blood enzymes (activated coagulation factor 13 and the Guinea pig hair follicle enzyme. J. Biol. Chem. *247*, 2798–2807.

Colombano, G., Travelli, C., Galli, U., Caldarelli, A., Chini, M.G., Canonico, P.L., Sorba, G., Bifulco, G., Tron, G.C., and Genazzani, A.A. (2010). A novel potent nicotinamide phosphoribosyltransferase inhibitor synthesized via click chemistry. J. Med. Chem. *53*, 616–623.

Dull, T., Zufferey, R., Kelly, M., Mandel, R.J., Nguyen, M., Trono, D., and Naldini, L. (1998). A third-generation lentivirus vector with a conditional packaging system. J. Virol. *72*, 8463–8471.

Enomoto, M., Bunge, M.B., and Tsoulfas, P. (2013). A multifunctional neurotrophin with reduced affinity to p75NTR enhances transplanted Schwann cell survival and axon growth after spinal cord injury. Exp. Neurol. *248*, 170–182.

Fraga, H., and Fontes, R. (2011). Enzymatic synthesis of mono and dinucleoside polyphosphates. Biochim. Biophys. Acta *1810*, 1195–1204.

Fukuhara, A., Matsuda, M., Nishizawa, M., Segawa, K., Tanaka, M., Kishimoto, K., Matsuki, Y., Murakami, M., Ichisaka, T., Murakami, H., et al. (2005). Visfatin: a protein secreted by visceral fat that mimics the effects of insulin. Science *307*, 426–430.

Galassi, L., Di Stefano, M., Brunetti, L., Orsomando, G., Amici, A., Ruggieri, S., and Magni, G. (2012). Characterization of human nicotinate phosphoribosyltransferase: kinetic studies, structure prediction and functional analysis by site-directed mutagenesis. Biochimie *94*, 300–309.

Galli, U., Travelli, C., Massarotti, A., Fakhfouri, G., Rahimian, R., Tron, G.C., and Genazzani, A.A. (2013). Medicinal chemistry of nicotinamide phosphoribosyltransferase (NAMPT) inhibitors. J. Med. Chem. *56*, 6279–6296.

Garten, A., Schuster, S., Penke, M., Gorski, T., de Giorgis, T., and Kiess, W. (2015). Physiological and pathophysiological roles of NAMPT and NAD metabolism. Nat. Rev. Endocrinol. *11*, 535–546.

Gholson, R.K., Ueda, I., Ogasawara, N., and Henderson, L.M. (1964). The enzymatic conversion of quinolinate to nicotinic acid mononucleotide in mammalian liver. J. Biol. Chem. *239*, 1208–1214.

Grolla, A.A., Torretta, S., Gnemmi, I., Amoruso, A., Orsomando, G., Gatti, M., Caldarelli, A., Lim, D., Penengo, L., Brunelleschi, S., et al. (2015). Nicotinamide phosphoribosyltransferase (NAMPT/PBEF/visfatin) is a tumoural cytokine released from melanoma. Pigment Cell Melanoma Res. *28*, 718–729.

Grolla, A.A., Travelli, C., Genazzani, A.A., and Sethi, J.K. (2016). Extracellular nicotinamide phosphoribosyltransferase, a new cancer metabokine. Br. J. Pharmacol. *173*, 2182–2194.

Gross, J., Rajavel, M., Segura, E., and Grubmeyer, C. (1996). Energy coupling in *Salmonella typhimurium* nicotinic acid phosphoribosyltransferase: identification of His-219 as site of phosphorylation. Biochemistry *35*, 3917–3924.

Gross, J.W., Rajavel, M., and Grubmeyer, C. (1998). Kinetic mechanism of nicotinic acid phosphoribosyltransferase: implications for energy coupling. Biochemistry *37*, 4189–4199.

Grubmeyer, C.T., Gross, J.W., and Rajavel, M. (1999). Energy coupling through molecular discrimination: nicotinate phosphoribosyltransferase. Methods Enzymol. *308*, 28–48.

Gunther Sillero, M.A., de Diego, A., Silles, E., and Sillero, A. (2005). Synthesis of (di)nucleoside polyphosphates by the ubiquitin activating enzyme E1. FEBS Lett. *579*, 6223–6229.

Hara, N., Yamada, K., Shibata, T., Osago, H., Hashimoto, T., and Tsuchiya, M. (2007). Elevation of cellular NAD levels by nicotinic acid and involvement of nicotinic acid phosphoribosyltransferase in human cells. J. Biol. Chem. *282*, 24574–24582.

Hara, N., Yamada, K., Shibata, T., Osago, H., and Tsuchiya, M. (2011). Nicotinamide phosphoribosyltransferase/visfatin does not catalyze nicotinamide mononucleotide formation in blood plasma. PLoS One *6*, e22781.

Hess, H.H., and Derr, J.E. (1975). Assay of inorganic and organic phosphorus in the 0.1-5 nanomole range. Anal. Biochem. *63*, 607–613.

Honjo, T., Nakamura, S., Nishizuka, Y., and Hayaishi, O. (1966). Stoichiometric utilization of adenosine 5'-triphosphate in nicotinate ribonucleotide synthesis from nicotinate and 5-phosphoribosyl-1-pyrophosphate. Biochem. Biophys. Res. Commun. *25*, 199–204.

Huang, D., Zhang, Y., and Chen, X. (2003). Analysis of intracellular nucleoside triphosphate levels in normal and tumor cell lines by high-performance liquid chromatography. J. Chromatogr. B Analyt Technol. Biomed. Life Sci. *784*, 101–109.

Imai, S. (2009). Nicotinamide phosphoribosyltransferase (Nampt): a link between NAD biology, metabolism, and diseases. Curr. Pharm. Des. *15*, 20–28.

Khan, J.A., Tao, X., and Tong, L. (2006). Molecular basis for the inhibition of human NMPRTase, a novel target for anticancer agents. Nat. Struct. Mol. Biol. *13*, 582–588.

Kosaka, A., Spivey, H.O., and Gholson, R.K. (1971). Nicotinate phosphoribosyltransferase of yeast. Purification and properties. J. Biol. Chem. *246*, 3277–3283.

Li, Y., Zhang, Y., Dorweiler, B., Cui, D., Wang, T., Woo, C.W., Brunkan, C.S., Wolberger, C., Imai, S., and Tabas, I. (2008). Extracellular Nampt promotes macrophage survival via a nonenzymatic interleukin-6/STAT3 signaling mechanism. J. Biol. Chem. *283*, 34833–34843.

Magni, G., Orsomando, G., Raffelli, N., and Ruggieri, S. (2008). Enzymology of mammalian NAD metabolism in health and disease. Front Biosci. *13*, 6135–6154.

Magni, G., Di Stefano, M., Orsomando, G., Raffaelli, N., and Ruggieri, S. (2009). NAD(P) biosynthesis enzymes as potential targets for selective drug design. Curr. Med. Chem. *16*, 1372–1390.

Maldi, E., Travelli, C., Caldarelli, A., Agazzone, N., Cintura, S., Galli, U., Scatolini, M., Ostano, P., Miglino, B., Chiorino, G., et al. (2013). Nicotinamide phosphoribosyltransferase (NAMPT) is over-expressed in melanoma lesions. Pigment Cell Melanoma Res. *26*, 144–146.

Marletta, A.S., Massarotti, A., Orsomando, G., Magni, G., Rizzi, M., and Garavaglia, S. (2015). Crystal structure of human nicotinic acid phosphoribosyltransferase. FEBS Open Bio. *5*, 419–428.

Marrian, D.H. (1954). A new adenine nucleotide. Biochim. Biophys. Acta *13*, 278–281.

Mori, V., Amici, A., Mazzola, F., Di Stefano, M., Conforti, L., Magni, G., Ruggieri, S., Raffaelli, N., and Orsomando, G. (2014). Metabolic profiling of alternative NAD biosynthetic routes in mouse tissues. PLoS One *9*, e113939.

North, R.A. (2016). P2X receptors. Philos. Trans. R. Soc. Lond. B Biol. Sci *371*, pii: 20150427.

Orsomando, G., Cialabrini, L., Amici, A., Mazzola, F., Ruggieri, S., Conforti, L., Janeckova, L., Coleman, M.P., and Magni, G. (2012). Simultaneous single-sample determination of NMNAT isozyme activities in mouse tissues. PLoS One *7*, e53271.

Pintor, J., Pelaez, T., and Peral, A. (2004). Adenosine tetraphosphate, Ap4, a physiological regulator of intraocular pressure in normotensive rabbit eyes. J. Pharmacol. Exp. Ther. *308*, 468–473.

Rajavel, M., Lalo, D., Gross, J.W., and Grubmeyer, C. (1998). Conversion of a cosubstrate to an inhibitor: phosphorylation mutants of nicotinic acid phosphoribosyltransferase. Biochemistry *37*, 4181–4188.

Ramsey, K.M., Yoshino, J., Brace, C.S., Abrassart, D., Kobayashi, Y., Marcheva, B., Hong, H.K., Chong, J.L., Buhr, E.D., Lee, C., et al. (2009). Circadian clock feedback cycle through NAMPT-mediated NAD+ biosynthesis. Science *324*, 651–654.

Rehan, L., Laszki-Szczachor, K., Sobieszczanska, M., and Polak-Jonkisz, D. (2014). SIRT1 and NAD as regulators of ageing. Life Sci. *105*, 1–6.

Retailleau, P., Weinreb, V., Hu, M., and Carter, C.W., Jr. (2007). Crystal structure of tryptophanyl-tRNA synthetase complexed with adenosine-5' tetraphosphate: evidence for distributed use of catalytic binding energy in amino acid activation by class I aminoacyl-tRNA synthetases. J. Mol. Biol. *369*, 108–128.

Revollo, J.R., Grimm, A.A., and Imai, S. (2004). The NAD biosynthesis pathway mediated by nicotinamide phosphoribosyltransferase regulates Sir2 activity in mammalian cells. J. Biol. Chem. *279*, 50754–50763.

Ruggieri, S., Orsomando, G., Sorci, L., and Raffaelli, N. (2015). Regulation of NAD biosynthetic enzymes modulates NAD-sensing processes to shape mammalian cell physiology under varying biological cues. Biochim. Biophys. Acta *1854*, 1138–1149.

Samal, B., Sun, Y., Stearns, G., Xie, C., Suggs, S., and McNiece, I. (1994). Cloning and characterization of the cDNA encoding a novel human pre-B-cell colony-enhancing factor. Mol. Cell Biol *14*, 1431–1437.

Shackelford, R.E., Mayhall, K., Maxwell, N.M., Kandil, E., and Coppola, D. (2013). Nicotinamide phosphoribosyltransferase in malignancy: a review. Genes Cancer *4*, 447–456.

Shimosaka, M., Fukuda, Y., Murata, K., and Kimura, A. (1985). Purification and properties of orotate phosphoribosyltransferases from *Escherichia coli* K-12, and its derivative purine-sensitive mutant. J. Biochem. *98*, 1689–1697.

Skokowa, J., Lan, D., Thakur, B.K., Wang, F., Gupta, K., Cario, G., Brechlin, A.M., Schambach, A., Hinrichsen, L., Meyer, G., et al. (2009). NAMPT is essential for the G-CSF-induced myeloid differentiation via a NAD(+)-sirtuin-1-dependent pathway. Nat. Med. *15*, 151–158.

Sorci, L., Blaby, I., De Ingeniis, J., Gerdes, S., Raffaelli, N., de Crecy Lagard, V., and Osterman, A. (2010). Genomics-driven reconstruction of acinetobacter NAD metabolism: insights for antibacterial target selection. J. Biol. Chem. *285*, 39490–39499.

Sorci, L., Blaby, I.K., Rodionova, I.A., De Ingeniis, J., Tkachenko, S., de Crecy-Lagard, V., and Osterman, A.L. (2013). Quinolinate salvage and insights for targeting NAD biosynthesis in group A streptococci. J. Bacteriol. *195*, 726–732.

Sukalski, K.A., and Nordlie, R.C. (1989). Glucose-6-phosphatase: two concepts of membrane-function relationship. Adv. Enzymol. Relat. Areas Mol. Biol. *62*, 93–117.

Sun, Z., Lei, H., and Zhang, Z. (2013). Pre-B cell colony enhancing factor (PBEF), a cytokine with multiple physiological functions. Cytokine Growth Factor Rev. *24*, 433–442.

Tolle, M., Jankowski, V., Schuchardt, M., Wiedon, A., Huang, T., Hub, F., Kowalska, J., Jemielity, J., Guranowski, A., Loddenkemper, C., et al. (2008). Adenosine 5'-tetraphosphate is a highly potent purinergic endothelium-derived vasoconstrictor. Circ. Res. *103*, 1100–1108.

Vinitsky, A., and Grubmeyer, C. (1993). A new paradigm for biochemical energy coupling. *Salmonella typhimurium* nicotinate phosphoribosyltransferase. J. Biol. Chem. *268*, 26004–26010.

Wang, T., Zhang, X., Bheda, P., Revollo, J.R., Imai, S., and Wolberger, C. (2006). Structure of Nampt/PBEF/visfatin, a mammalian NAD+ biosynthetic enzyme. Nat. Struct. Mol. Biol. *13*, 661–662.

Yoon, M.J., Yoshida, M., Johnson, S., Takikawa, A., Usui, I., Tobe, K., Nakagawa, T., Yoshino, J., and Imai, S. (2015). SIRT1-mediated eNAMPT secretion from adipose tissue regulates hypothalamic NAD+ and function in mice. Cell Metab. *21*, 706–717.

Zamporlini, F., Ruggieri, S., Mazzola, F., Amici, A., Orsomando, G., and Raffaelli, N. (2014). Novel assay for simultaneous measurement of pyridine mononucleotides synthesizing activities allows dissection of the NAD(+) biosynthetic machinery in mammalian cells. FEBS J. *281*, 5104–5119.

Zhao, Y., Liu, X.Z., Tian, W.W., Guan, Y.F., Wang, P., and Miao, C.Y. (2014). Extracellular visfatin has nicotinamide phosphoribosyltransferase enzymatic activity and is neuroprotective against ischemic injury. CNS Neurosci. Ther. *20*, 539–547.

STAR★METHODS

KEY RESOURCES TABLE

REAGENT or RESOURCE	SOURCE	IDENTIFIER
Antibodies		
Anti-Nampt (Visfatin/PBEF), mAb (OMNI379)	AdipoGen	Cat#AG20A0034; RRID: AB_2490117
Anti-β-Actin, Mouse monoclonal	Sigma-Aldrich	Cat#A1978; RRID: AB_476692
Goat Anti-Mouse IgG-HRP Conjugate	Bio-Rad	Cat#1706516; RRID: AB_11125547
Bacterial and Virus Strains		
One Shot BL21 Star (DE3) Chemically Competent *E. coli* cells	Invitrogen	Cat#440049
Chemicals, Peptides, and Recombinant Proteins		
Adenosine-5'-tetraphosphate (Ap4) (~95% pure)	Jena Bioscience	Cat#NU1102
FK866	Colombano et al., 2010	N/A
TALON metal affinity resin	Clonetech	Cat#635502
PD-10 desalting columns (Sephadex G-25)	GE Healthcare	Cat#17085101
Tris(2-carboxyethyl)phosphine HCl (TCEP)	Sigma-Aldrich	Cat#75259
Isopropyl β-D-1-thiogalactopyranoside (IPTG)	Sigma-Aldrich	Cat#I6758
Nonidet P-40 Substitute	Fluka	Cat#74385
Dulbecco's Modified Eagle's Medium - high glucose (DMEM)	Sigma-Aldrich	Cat#D5671
Minimum Essential Medium Eagle (MEM)	Sigma-Aldrich	Cat#M5650
Fetal bovine serum (FBS)	Gibco	Cat#10270106
L-Glutamine	Sigma-Aldrich	Cat#G7513
Penicillin/streptomycin	Sigma-Aldrich	Cat#P0781
Biomol Green reagent (Malachite assay)	Enzo Life Sciences	Cat#BMLAK111
Bradford reagent	Sigma-Aldrich	Cat#B6916
Pierce BCA Protein Assay Kit	Thermo Fisher Scientific	Cat#23227
Protease Inhibitor Cocktail (Set VI)	Calbiochem	Cat#539133
Phenylmethanesulfonyl fluoride (PMSF)	Fluka	Cat#78830
Calf intestine alkaline phosphatase (with buffer)	Fermentas	Cat#EF0341
Crotalus adamanteus phosphodiesterase I	Sigma-Aldrich	Cat#P3134
Alcohol dehydrogenase (ADH)	Sigma-Aldrich	Cat#A7011
Recombinant *E. coli* NMN deamidase (PncC)	Zamporlini et al., 2014	N/A
Recombinant *B. anthracis* NaMN adenylyltransferase (NadD)	Zamporlini et al., 2014	N/A
Recombinant *B. anthracis* NAD synthetase (NadE)	Zamporlini et al., 2014	N/A
Recombinant Mouse NAMPT & its H247E mutant	Grolla et al., 2015	N/A
Recombinant Human NAPT & its H213A mutant	Galassi et al., 2012	N/A
Recombinant *A. baylyi* NAMPT (NadV)	Sorci et al., 2010	N/A
Recombinant *S. aureus* NAPT (PncB)	This study	N/A
Recombinant *S. pyogenes* Quinolinate PRTase (NadC)	Sorci et al., 2013	N/A
Critical Commercial Assays		
Nampt (Visfatin/PBEF) (mouse/rat) Dual ELISA Kit	AdipoGen	Cat#AG45A0007YEK-KI01
Experimental Models: Cell Lines		
B16-F0 (mouse melanoma)	ATCC	Cat#CRL6322
B16 FLAG-NAMPT (over-expressing NAMPT)	Grolla et al., 2015	N/A
B16 shNAMPT Low (silencing NAMPT)	Grolla et al., 2015	N/A
HEK293T (lentiviral particles assembly)	ATCC	Cat#CRL3216

(*Continued on next page*)

Continued

REAGENT or RESOURCE	SOURCE	IDENTIFIER
Experimental Models: Organisms/Strains		
Mouse: C57BL/6 (plasma collection)	Charles River	Strain code 027
Recombinant DNA		
pLV-IRES-GFP	Enomoto et al., 2013	Addgene Plasmid #36083
pMDLg/pRRE	Dull et al., 1998	Addgene Plasmid #12251
pMD2.VSVG	gift from Didier Trono	Addgene Plasmid #12259
pRSV-Rev	Dull et al., 1998	Addgene Plasmid #12253
pLV-FLAG-NAMPT-IRES-GFP	Grolla et al., 2015	N/A
GIPZ Mouse Nampt Lentiviral shRNA	GE Dharmacon	Cat# V3LMM_518294
Plasmid constructs for recombinant His-tag PRTases expression provided in Table S1		
Software and Algorithms		
GraphPad PRISM v4.0c for Macintosh	GraphPad Software, Inc.	GPM4-040637-RDE-3782
Xcalibur® v2.0.7 SP1	Thermo Fischer Scientific	N/A
Quantity One v4.6.9	Bio-Rad	Cat#1709600

CONTACT FOR REAGENT AND RESOURCE SHARING

Further information and requests for resources and reagents should be directed to and will be fulfilled by the Lead Contact, Giuseppe Orsomando (g.orsomando@univpm.it).

EXPERIMENTAL MODEL AND SUBJECT DETAILS

Cell Lines

B16 cells were engineered for NAMPT over-expression or silencing as follows. To generate a stable B16 FLAG-NAMPT cell line over-expressing NAMPT, a FLAG-NAMPT was cloned in the pLV-IRES-GFP bicistronic vector (Enomoto et al., 2013). The lentiviral particles were produced in HEK293T cells transfected with pMDLg/pRRE, pMD2.VSVG, pRSV-Rev (Dull et al., 1998), and pLV-FLAG-NAMPT-IRES-GFP. Briefly, after 48 h, the cell medium was collected, filtrated, and centrifuged at 100,000×*g* for 90 min. The viral particles in the pellet fraction were titrated, resuspended at appropriate concentrations, and used to infect B16 cells. Likewise, a stable B16 shNAMPT Low cell line silencing NAMPT was obtained after B16 infection with lentiviral particles. These particles were produced as described above in HEK293T cells by using a second-generation packaging plasmid system added with GIPZ Mouse Nampt Lentiviral shRNA plasmid. The infected cells were sorted for high levels of GFP (GFP++, called B16 shNAMPT Low cells).

All B16 cells were normally cultured in DMEM supplemented with 10 % fetal bovine serum (FBS), 2 mg/mL glutamine, 10 U/mL penicillin and 100 lg/mL streptomycin. Typically, 1.5×10^6 cells were seeded and detached after 24 hours by trypsinization. When required, B16 cells were treated for 24 hours with 100 nM FK866. IC50 for FK866 on these cells is 122 nM at 72 hours. For metabolism perturbation, cells were grown for 20 hours after adhesion in DMEM (4.5 g/L glucose) ± FBS, or MEM (1.0 g/L glucose) ± FBS.

Animals

Eight weeks old C57BL/6 healthy male mice were grown and treated under procedures authorized by the animal ethical committee of the University of ''Piemonte Orientale'' (Novara, Italy).

METHOD DETAILS

Preparative HPLC Chromatography

The Ap4 from Jena Bioscience or from the ATPase assays described below was purified by HPLC onto a Tosoh Bioscience TSKgel DEAE-2SW (250 × 46 mm) column. Elution was carried out at room temperature in volatile buffers, ammonium acetate 0.05 M (A) and 1 M (B), at pH 5.5. The gradient applied at 1 mL/min flow rate was: 2.5 min at 25 % B; 23.5 min up to 60 % B; 2 min up to 100 % B; 4 min hold at 100 % B; 1 min down to 25 % B; 6 min hold at 25 % B. After subsequent injections of each sample in aliquots, the fractions corresponding to UV peaks eluting at ~22 min were pooled. The purified Ap4 was quantified from the Abs(260 nm) using an ε(260 nm) of 15.4 mM^{-1} cm^{-1}, then frozen and lyophilized.

Chemical and Enzymatic Digestion of the Purified NAMPT Product

Following preparative HPLC chromatography, Ap4 amounts of 0.5, 1 and 2 nmol appropriately lyophilized in cleaned, acid-washed glass tubes, were ashed in a magnesium nitrate/ethanol solution (Hess and Derr, 1975), before the chemically released organic Pi was quantified by Malachite green. A reference curve was created by treating in parallel pure ATP, ADP, and AMP (0.5 to 3 nmol each, from UV calibrated solutions). Alternatively, enzymatic digestions were carried out in either 0.3 mL mixtures containing ~0.4 U/mL calf intestine alkaline phosphatase in the supplied buffer, or 0.2 mL mixtures containing 0.04 mU/mL *Crotalus adamanteus* phosphodiesterase I in 0.1 M Tris/HCl buffer, pH 8.9, 0.1 M NaCl, 15 mM $MgCl_2$. The mixtures contained 20-40 μM of purified Ap4 and were treated and analysed by C18-HPLC (see *Activity assays)*. The commercial phosphodiesterase used was contaminated by a 5'-nucleotidase activity.

Cloning, Expression, and Purification

The expression constructs used for mouse NAMPT and its H247E mutant are described in (Grolla et al., 2015), those for human NAPT and its H213A mutant in (Galassi et al., 2012), that for *Acinetobacter baylyi* NadV in (Sorci et al., 2010), and that for *Streptococcus pyogenes* NadC in (Sorci et al., 2013). The expression construct for *Staphylococcus aureus* PncB was obtained in this study by PCR amplification from genomic DNA and cloning into a pET-derived vector (see Table S1 for cloning details). Their transformation into *E. coli* BL21(D3) competent cells, expression by induction with IPTG 0.5 mM for 17h at 26-28 °C, and purification by TALON chromatography were carried out essentially as described (Orsomando et al., 2012). The purified enzymes were finally desalted on PD-10 in 50 mM HEPES/NaOH buffer, pH 7.5, 1 mM TCEP, and stored at -80 °C. Their concentration was measured by the Bradford reagent protein assay. All these recombinant proteins were fused to N-terminal and/or C-terminal His-tag tails (see Table S1).

Activity Assays

One unit (U) is defined as the enzyme amount catalyzing 1 μmol/min product formation (or substrate consumption) at 25 °C. Rates were calculated in the linear region of *v vs t* plots (product accumulation versus time). The PRTase activities of NAMPT and NAPT (either NMN or NaMN synthesis) were measured by adapting a continuous assay based on detection at 340 nm of the NADH formed (Balducci et al., 1995) in the presence of PncC, NadD, NadE, and ADH as the ancillary enzymes (Zamporlini et al., 2014). The mixtures for NAMPT assay contained, in 0.5 mL final volume, 80 mM HEPES/NaOH buffer, pH 7.5, 12 mM $MgCl_2$, 0.5 mg/mL bovine serum albumin, 75 mM ethanol, 30 mM semicarbazide, 4.5 mM NH_4Cl, 0.024 U/mL PncC, 0.192 U/mL NadD, 0.081 U/mL NadE, 12.5 U/mL ADH, 1 mM ATP, 0.5 mM PRPP, 0.5 mM Nam, and 20-40 μg/mL of enzyme to be tested. In NAPT assays, PncC was omitted, 50 mM K_2HPO_4, pH 7.5, was included in addition (Galassi et al., 2012), and Na 0.5 mM was used in place of Nam. The pyridine substrate was usually added to start the reaction and, when indicated, mixtures were supplied with 2.5 μL of 10 mM FK866 in DMSO (50 μM final). Alternatively, the ATPase activities of NAMPT and NAPT (either ADP or Pi or Ap4 synthesis) were measured by discontinuous assays. The assay mixtures contained, in 0.2 mL final volume, 50 mM HEPES/NaOH buffer, pH 7.5, 5 mM $MgCl_2$, from 0.25 to 2.5 mM ATP, and from 0.03 to 2.3 mg/mL each enzyme (*i.e.* 0.5-40 μM based on average MW in Table S1). The enzyme or ATP were added to start the reaction and, when indicated, mixtures were supplied with 1 μL of 10 mM FK866 in DMSO (50 μM final) or other compounds in water. During incubation, 20-μL aliquots were collected at different times and stopped on ice by addition of 10 μL $HClO_4$ 1.2 M. These aliquots were centrifuged, neutralized by addition of 6.8 μL K_2CO_3 1M, and centrifuged again. For analytical purposes, the supernatants were injected into HPLC for separation and UV detection of both ADP and Ap4 formed, or treated with Malachite Green for VIS detection of the Pi formed (Hess and Derr, 1975). In this latter case, they were quenched with two volumes of Biomol Green reagent, left for 15 min on the bench, and read at 620 nm. A calibrated solution of KH_2PO_4 was used for Pi quantitation. The HPLC analysis was carried out either by ion pair-reverse phase chromatography onto a Supelcosil LC18-S (250 × 46 mm) column as reported (Mori et al., 2014), or by the above anion exchange TSK-DEAE chromatography (see *Preparative HPLC*). Both HPLC methods allowed separation of Ap4, ATP, ADP, AMP, and adenosine, as verified by coelution with corresponding standards. The integrated peak areas were converted into nanomoles as described (Mori et al., 2014), using the ε(260 nm) of 15.4 mM^{-1} cm^{-1}. Both NMN and NaMN after C18-HPLC were likewise quantified using an ε(260 nm) of 3.5 mM^{-1} cm^{-1}.

Cell Extraction for Western Blot Analysis

To monitor NAMPT expression and stability in the engineered cell lines B16 FLAG-NAMPT and B16 shNAMPT Low, cultured cells were collected and lysed in a 20 mM HEPES/NaOH buffer, pH 7.5, containing 100 mM NaCl, 5 mM EDTA, 1 % Nonidet P-40, 1 mM PMSF, and appropriate aliquots of the Calbiochem Protease Inhibitor Cocktail Set VI. Proteins extracted were quantified by the BCA Protein Assay, separated on SDS-PAGE, blotted onto a nitrocellulose membrane, and stained with monoclonal antibodies specific for NAMPT and beta-Actin. Densitometry analysis was next performed with the Bio-Rad Quantity One program.

Cell Extraction for MS Analysis

The various B16 cells freshly grown and collected were frozen in liquid nitrogen and immediately lysed in 400 μL water/acetonitrile (1:3 vol/vol). Proteins were precipitated by centrifugation. The supernatant was treated in two different ways before LC-ESI-MS analysis. For quantification of Ap4, ATP and ADP, a 300 μL aliquot was evaporated in a rotational vacuum concentrator to dryness (for 4 h at 30 °C) and reconstituted in 80 μL water/acetonitrile (1:1 vol/vol). For quantification of Nam, NMN and NAD, 80 μL of supernatant were directly analysed. Values in nmol were referred to mg of protein extracted and quantified from the cell lysate.

Mouse Plasma Sampling and Treatment

From 3 mice, blood samples were drawn three times on separate days, while from other 14 mice, a single blood sample was collected. Before LC-ESI-MS analysis, 100 μL of plasma were added to 300 μL of methanol, clarified by centrifugation, and then a 320-μL aliquot was evaporated to dryness and reconstituted in 80 μL water/acetonitrile (1:1 vol/vol). In parallel, 100 μL of plasma without dilution were used to quantify the extracellular NAMPT content by means of the Nampt (Visfatin/PBEF) (mouse/rat) Dual ELISA Kit.

LC-ESI-MS analysis of Pyridine and Adenine Nucleotides

Analyses were carried out onto a Thermo Finnigan LCQ Deca XP Plus system equipped with a quaternary pump, a Surveyor AS autosampler, and a vacuum degasser (Thermo Finnigan). The liquid chromatography was performed on a Phenomenex Luna HILIC column (150 x 2 mm, 3μm) with a Phenomenex Luna HILIC security guard column (4 mm x 2 mm), at 25 °C, at 200 μL/min flow rate, under isocratic elution. The mobile phase was composed by a 70 : 30 ratio of acetonitrile and 100 mM ammonium acetate buffer, pH 5.8. The injection volume was 5 μL and the run time was 20 min. The MS detection was performed using two different methods: negative polarity for Ap4 (SRM m/z 586 > 488 C.I.D. 25 eV), ATP (SRM m/z 506 > 408 C.I.D. 25 eV), and ADP (SRM m/z 426 > 328 C.I.D. 30 eV), and positive polarity for Nam (MSMS m/z 123 C.I.D. 25 eV), NMN (SRM m/z 335 > 123 C.I.D. 25 eV), and NAD (MRM m/z 664 > 542, 524 C.I.D. 25 eV). The instrument was set as follows: ion spray voltage, 4 kV; source current, 80 μA; capillary temperature, 350 °C; sheath gas flow (N2), 60 Auxiliary Units (A.U.); sweep gas flow (N2): 6.0 A.U., capillary voltage, -15.00 V (negative polarity) and 18.00 V (positive polarity); tube lens offset, -5.0 V (negative polarity) and 10.00 V (positive polarity); multipole 1 offset, 7.50 V (negative polarity) and -5.00 V (positive polarity); multipole 2 offset, 11.00 V (negative polarity) and -8.00 V (positive polarity).

QUANTIFICATION AND STATISTICAL ANALYSIS

All data represent the mean and SEM or SD of at least 3 independent experiments. T test analysis was carried out by PRISM program. A p value ≤ 0.05 was considered as significant, and indicated in figures with asterisks (*). LC-MS data were acquired and processed using the Xcalibur® software. For quantification of Ap4, ATP, ADP, Nam, NMN and NAD in cell extracts and plasma samples, calibration curves in the appropriate range were prepared (external calibration method) with a correlation coefficient (R^2) always > 0,99; data were corrected for recovery and matrix effect when present.